ATLAS Internal Note
16 March 1999

Status Report on Cooling Activities involving the University of Geneva.

Gérard Barbier, Philippe Bouvier, Allan G. Clark, Eric Perrin, Maarten Weber

DPNC, Section de Physique, University of Geneva, Switzerland.

Michel Bosteels, Greg Hallewell

CERN, Geneva, Switzerland.

Abstract

A summary is made of recent activities at the University of Geneva towards a viable cooling design for the SCT barrel modules. Future plans are also described.

1.0 Introduction

The cooling studies carried out by the Geneva group have been directed towards an understanding of the thermal behaviour of barrel modules, and the demonstration of a performant and reliable contact between cooling fluids and the detector module.

Given that the silicon detectors are required to operate at approximately -7 ^{0}C following the radiation damage expected in ATLAS [1], and the need to maintain a uniform detector temperature over an extended period, the reliability of the cooling contact has some practical relevance.

An initial study of the cooling contact has already been completed using a full length cooling prototype [2]. Since that time, however, there have been several developments.

- The base-line design of Leakless cooling using binary ice has been abandoned [3], with as yet no final choice of the SCT cooling tube diameter or coolant. An over-pressure evaporative cooling design was recommended and is the preferred solution, using C_4F_{10}, CF_3I or C_3F_8 [4]. At the same time, an over pressure single phase fluorinert system was recommended as a viable backup. A high-pressure fluorinert [FC72] solution has already been demonstrated by Gildemeister [5] and others.
- The so-called z-module design which was used for the majority of studies in [2] has been replaced by a centre-tap design of the type also described in [2]. The most recent base-line centre tap module has in principle an improved electrical performance, but in order to reduce the material budget has a deteriorated thermal behaviour and a reduced cooling contact area with respect to both the z-module, and the original thermal centre tap design, fabricated and tested as in [2]).

Given the ongoing studies of evaporative cooling at CERN [4], the Geneva group has concentrated on complementary or support activities relevant to the SCT barrel cooling.

- In the work of [2], an oval Al cooling tube was developed, of 9.2 mm external width, 2 mm external thickness, and of 0.25 mm wall thickness. A sliding cooling contact was provided by the use of a 50 μm thick layer of Dow Corning DC340 conductive grease. This tube was tested using a Leakless single-phase methanol-water solution as part of a full-length prototype programme. The cooling system has since been adapted to provide over-pressure cooling via single-phase fluorinert coolant (C_6F_{14}), and cooling studies using the oval tube have been successfully repeated. This is described in Section 2.
- In order to reduce the service cross-section at the barrel-forward interface, the distribution of coolant via an entry manifold at the barrel end was suggested. A prototype 8-line manifold was constructed, and shown to operate satisfactorily in Leakless mode. The performance has now been measured in over-pressure mode, and shown to be satisfactory. These measurements are described in Section 3. At the request of the CERN group, the 8-line manifold has now been modified for use in evaporative mode.
- Single full-length round pipes of respectively 3.5 (4) mm and 1.45(1.8) mm internal (external) diameter have been prepared for evaporative measurements by the CERN group [6].
- A number of thermal modules have been built for thermal and metrology tests, as part of a revised full-length prototype study. Twelve modules have been fabricated using Cu plates, with a heat conduction and contact as for the beryllia/TPG/silicon base-line design. Four other modules are detailed replicas of the base-line module design. The thermal and mechanical behaviour of these modules, both individually and as part of a full-length prototype, are described in Section 4. In this latest study, the modules and

cooling tube are supported using prototype carbon fibre support brackets as in the base-line engineering design.

Following a final cooling decision, the full-length prototype will be adapted to the relevant base-line design (Section 5).

2.0 Cooling studies with a single tube, using single-phase fluorinert (C_6F_{14}) or aqueous solutions.

Single phase cooling at high pressure in small diameter cooling tubes is the base-line cooling scheme of the CMS collaboration, and was previously proposed and demonstrated by Gildemeister [5]. The choice of small diameter tubes is attractive, especially in the forward direction, and remains a viable cooling option.

However, in the barrel, the existing oval cooling tube has a potential advantage of providing a large cooling contact to barrel modules and opto-boards. A request was made to study the feasibility of single phase fluorinert cooling using the existing pipe shape, and only a limited over-pressure.

2.1 Characteristics of the cooling unit, and coolants.

The 2 kW cooling unit was converted by the group of M. Bosteels from Leakless to over-pressure operation using either fluorinert or aqueous (glycol-water and methanol-water) coolants. The unit now provides a flow rate of up to 120 l/hr, at a pressure (for aqueous solutions) of up to 2 bars. An operating temperature range of $-20 < T < 5\ ^oC$ is possible using the current unit.

2.2 Cooling Pipe description and measurements

The 1.6 m long oval tube described in [3] and shown in Figure 1 was used. A heater element dissipated 60 Watts along the length of the pipe. PT100 heat sensors, which were glued to the pipe inlet and outlet, were used to record the temperature. A drawing of the cooling pipe is shown in Figure 1. Measurements (Table 1) of the cooling power were made using both aqueous and fluorinert coolants, at an ambient temperature of ~ $-10\ ^oC$. A simple theoretical model was able to reproduce the temperature difference between pipe inlet and outlet.

A direct comparison of these data with that measured in Leakless operation is also shown in Table 1. At approximately 3 times the flow rate required for Leakless operation, an equivalent cooling power can be obtained. Because of the poor thermal capacity of C_6F_{14} as compared with water-based coolants, a single-tube flow rate of 47 l/hr is required.

The above measurements translate to a flow rate of ~ 300 l/hr, for operation using an 8-fold inlet manifold. The implications of this for a large system should not be underestimated. Similarly, a significantly larger heat load would result in an unacceptable temperature drop along the tube, exceeding the nominal specification of ~2-3 ^oC.

Coolant Liquid	T_{in}	T_{out}	T_{air}	Flow l/hr (cm^3/sec)	ΔP (mbar)	ΔT (^oC) (theory)
Water/ ethylene glycol (leakless)	-9.4	-5.3	-10.7	13.6 (3.8)	310	4.1 (4.2)
Water/ methanol (leakless)	-9.8	-7.4	-10.1	22.3 (6.2)	283	2.4 (2.5)
C_6F_{14}	-9.6	-7.1	-10.5	47.6 (13.2)	288	2.5 (2.6)

TABLE 1. Measurements of the cooling power of an aluminium cooling tube as described in the text and Figure 1. Shown in brackets are the flow rates for leakless cooling (column 5) and of theoretical simulations (column 7).

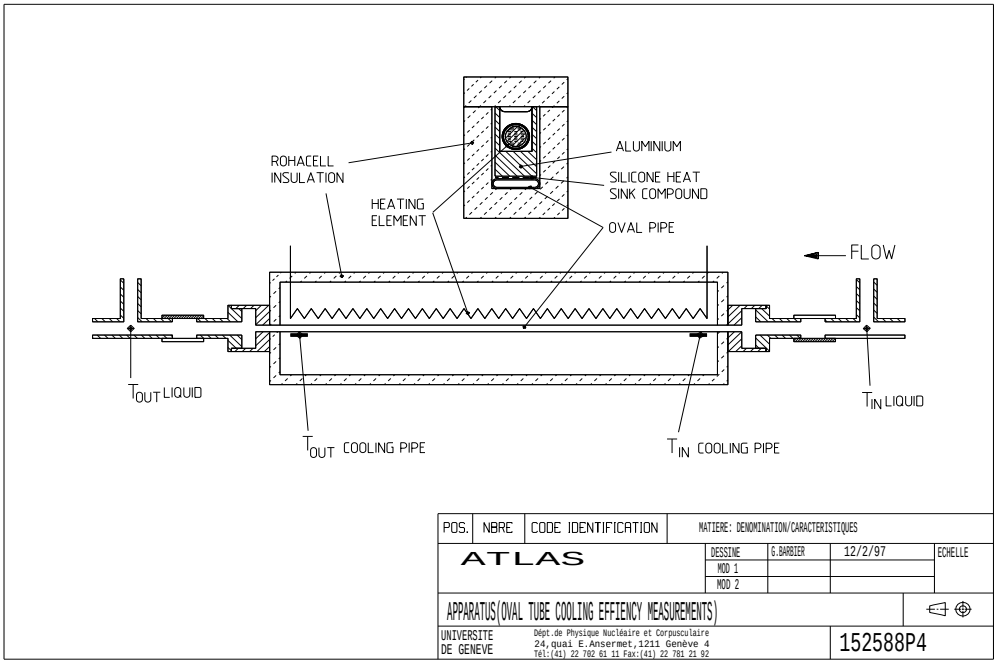

FIGURE 1. Drawing of the single cooling pipe used for cooling power measurements.

3.0 The use of a inlet and outlet manifold.

In the case of Leakless cooling, an inlet and/or outlet manifold was considered in order to reduce the service and material budget of the SCT. An 8-fold manifold, which is shown in Figure 2, was constructed using identical cooling tubes to that described in Section 2.

Each tube was fitted with a heating element, and with PT100 temperature sensors at the tube inlet and outlet.

The both the inlet and outlet of the manifold had an internal diameter of 12 mm.

Using a heat load of 60 W on each tube (480 W total), and a water-methanol solution (24% methanol by weight), the data of Table 2 and Figure 3 were measured. The temperature increase along each tube was measured to be ~ 3.5 ^{0}C, with a rms variation of only 0.164 ^{o}C. Variations of up to 0.9 ^{o}C in the absolute T_{in} and T_{out} values are thought to result from tube-to-tube flow variations. The larger temperature difference, as compared with Table 1, resulted from a reduced flow rate.

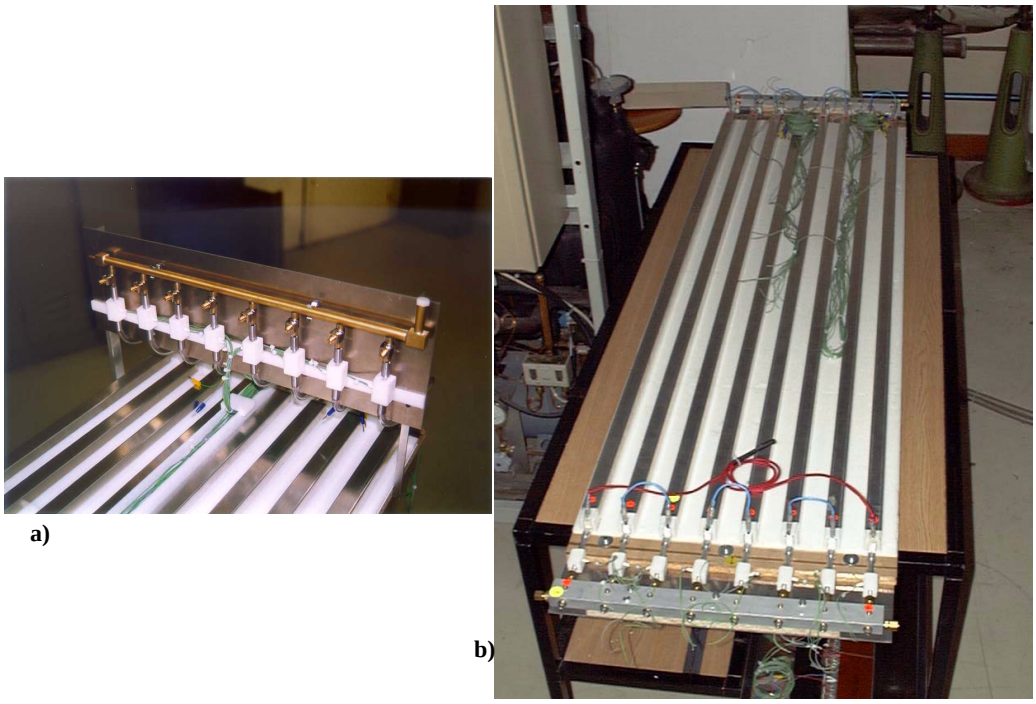

a)

b)

FIGURE 2. Photograph of 8-fold inlet manifold used for heat load studies. (a) shows the source manifold of internal diameter 12 mm, and (b) shows the full manifold after the addition of rubies for evaporative measurements [6].

Coolant: methanol (24),-water ΔP : ~ 300 mbars			
Tube #	**T_{in} °C**	**T_{out} °C**	**ΔT°C**
1	-7.56	-3.92	-3.6
2	-7.12	-3.85	-3.3
3	-7.1	-3.83	-3.3
4	-7.38	-4.1	-3.3
5	-7.6	-3.9	-3.7
6	-7.9	-4.4	-3.5
7	-7.8	-4.1	-3.7
8	-7.99	-4.58	-3.4
rms	0.34	0.27	0.164

TABLE 2. Measurements of the temperature at tube inlet and outlet for the 8-fold manifold. The larger temperature difference, as compared with Table 1, is due to a reduced flow rate (15 l/hr).

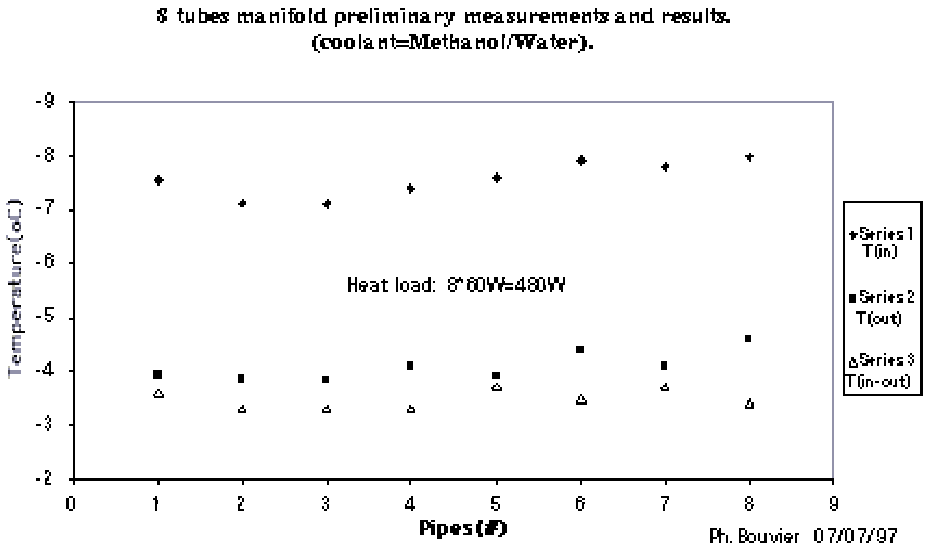

FIGURE 3. Measurements of the input and output temperatures for an 8-fold manifold.

Measurements using this manifold were limited, because of its conversion to evaporative mode by the gluing of rubies (0.3 mm holes) at the inlet to each tube. Results in this mode are reported separately [8].

4.0 Module construction and performance.

A number of thermal 'replicas' of the barrel modules have been constructed, with the eventual aim of making a full-length prototype test of the cooling on the barrel, using the final module design, the final cooling system, and the final mechanical arrangement.

At the present time, 12 Cu-based modules have been fabricated, as well as 3 thermal modules using the exact construction materials of the base-line centre-tap module. Each module has been tested (Section 4.2) on the 'single module' test stand which is described in Section 4.1. The modules have then been included in the full-length prototype tests.

A fourth thermal module using irradiated detectors will be fabricated. It would be valuable to test modules fabricated in other institutes.

4.1 Single module test stand.

Figure 4 shows a photograph of the single-module test stand, with a prototype thermal module attached (this is module C-4 described in Section 4.3. The stand consists of 250 mm length aluminium cooling tube having the previously described dimensions, and mounted onto a carbon-fibre base-plate. PT100 temperature probes which are glued to the tube measure T_{in} and T_{out}.

Individual modules can be attached to this stand, with thermal contact to the cooling tube via a 50 μm layer of DC340.

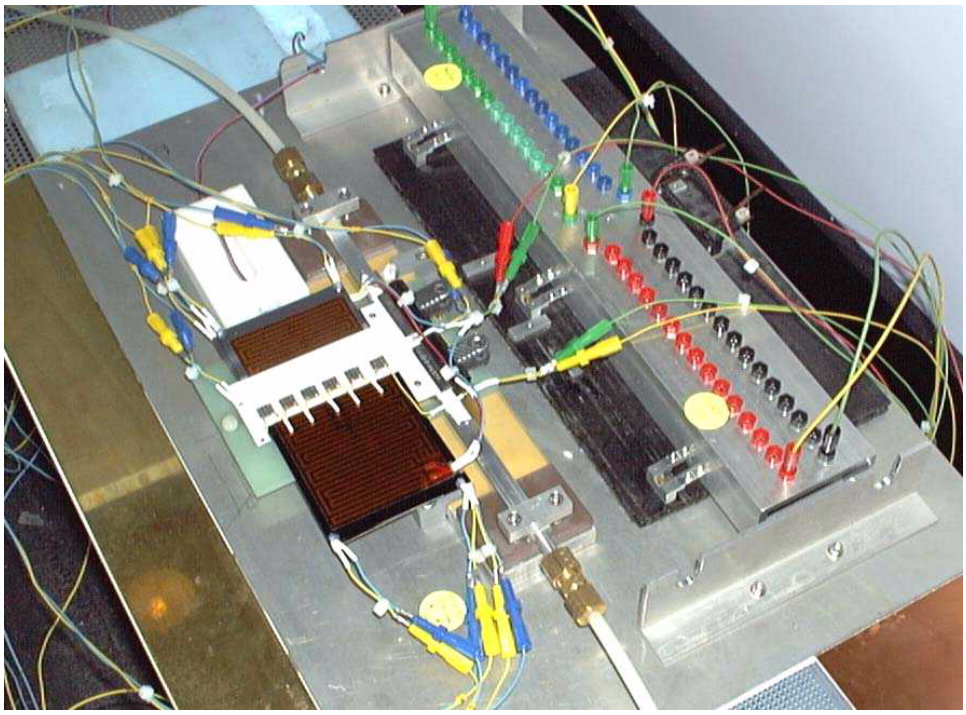

FIGURE 4. Photograph of single-module test stand, with the silicon-TPG module C-4 attached.

4.2 Thermal module prototypes - Cu plates -construction and results.

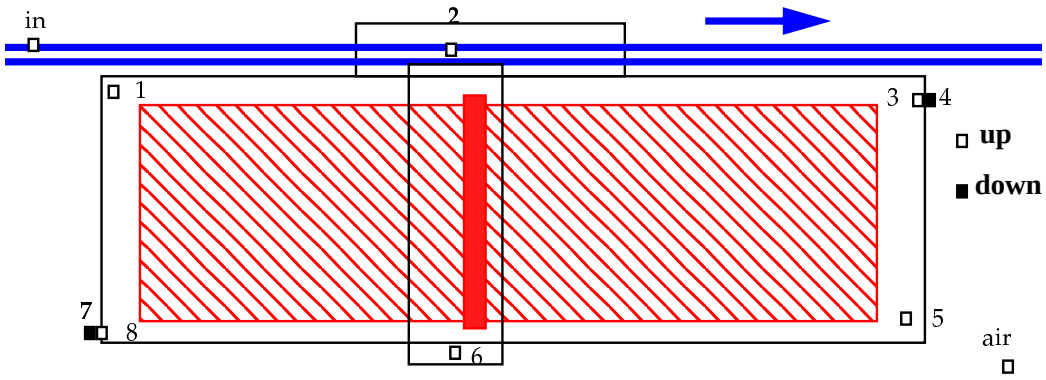

FIGURE 5. Schematic of the Cu-based thermal modules used for the full-length prototype tests.

Figure 5 shows the layout of the Cu-based modules (type Cu-A), which have the following characteristics. The overall dimensions (63.6 x 128 mm^2) are exactly that of the base-line modules, and the Cu-thickness of 1.5 mm has been chosen to give the same mean in-plane heat conduction as the base-line modules. Two separate Cu plates (74.6 x 28 x 0.4 mm^3), separated from the main Cu plate by 0.3 mm spacers, simulate the BeO hybrids, and electronic power is simulated by a heater pad covering the nominal front end chip positions. A heater blanket of size 114 x 57 mm^2, glued on the upper side of the main Cu plate, provides a heat load equivalent to that of an irradiated module. A total of 12 such modules have been constructed. On one module, PT100 sensors have been installed at positions 1 through 8 as shown in Figure 5. On the other modules, position 5 has been equipped (in some cases on the lower side of the plate because of space castrates for lower modules on the full-length prototype).

Each module has been attached in turn to the single module test stand, with an ~50 µm grease contact to the cooling pipe. Cooling measurements were made with a heat load of 4W for the heater resistors modelling the hybrid, and between 0.5 and 1.5 W for the 'detector' heater blankets. Results for the temperature probe 5 are shown in Table 3. The module-to-module differences are within the granularity of the temperature measurement (the grease cooling contact was in all cases maintained using clips).

Thermal Losses

A comparison has been made between the single-plate Cu module of 1.5 mm thickness (A) with the heater elements on the upper surface of the plate and the double-plate Cu module of 2 x 0.7 mm thickness with the heater element between the plates (B). This comparison provides a good estimate of the temperature correction required for radiation effects, in these modules.

Cooling measurements were made with a heat load of 4W for the heater resistors modelling the hybrid, and between 0.5 and 1.5 W for the 'detector' heater blankets.

Coolant: C_6F_{14} **Coolant flow:** *48 l/hr* **ΔP (mbars):** *~ 300*				
Module #	**$T_{in/out}$ ^oC**	**T (probe 5) ^oC P_{sensor}= 0.5 W P_{elect} = 4 W**	**T (probe 5) ^oC P_{sensor}= 1.0 W P_{elect} = 4 W**	**T (probe 5) ^oC P_{sensor}= 1.5 W P_{elect} = 4 W**
A-1	-10.03/-9.51	-5.11	-3.81	-3.29
A-2	"	-4.85	-3.55	-3.03
A-3	-9.77/-9.51	-4.85	-3.81	-3.03
A-4	-10.03/-9.77	-5.11	-4.01	-3.29
A-5	"	-4.85	-3.81	-3.03
A-6	"	-4.85	-3.81	-3.16
A-7	"	-4.85	-3.81	-3.16
A-8	"	-4.85	-3.81	-3.29
A-9	-10.03/-9.64	-5.1	-4.01	-3.16
A-10	-10.03/-9.77	-4.59	-3.55	-2.77
A-11	"	-4.85	-3.55	-2.77
A-12	"	-5.11	-3.81	-3.03

TABLE 3. Test of uniformity of the 12 Cu-based thermal modules. The reproducibility of successive modules is maintained to within the temperature measurement granularity.

Table 4 shows the temperature profile of the PT100 sensors 1, 2, 5 and 6. Excepting at very high sensor heat load, the temperature difference was ~ 0.25 ^oC.

Detector Power (W)	**Temp ^0C Sensor 1 Cu-A(B)**	**ΔT (^oC)**	**Temp ^0C Sensor 2 Cu-A(B)**	**ΔT (^oC)**	**Temp ^0C Sensor 5 Cu-A(B)**	**ΔT (^oC)**	**Temp ^0C Sensor 6 Cu-A(B)**	**ΔT (^oC)**
0.50	-4.85 (-4.6)	**-0.25**	-6.1 (-6.1)	**0.**	-4.32 (-4.32)	**0.0**	-2.77 (-2.51)	**-0.26**
0.75	-4.32 (-4.07)	**-0.25**	-5.62 (-5.62)	**0.**	-4.07 (-3.81)	**-0.26**	-2.51 (-2.25)	**-0.26**
1.0	-3.81 (-3.55)	**-0.26**	-5.1 (-5.4)	**+0.3**	-3.29 (-3.0)	**-0.29**	-1.70 (-1.50)	**-0.20**
1.5	-3.3 (-2.77)	**-0.53**	-5.1 (-4.85)	**-0.25**	-2.77 (-2.26)	**-0.51**	-1.2 (-0.7)	**-0.50**

TABLE 4. Temperature comparison of a Cu thermal module with a single heater element on the surface of 1.5 mm plate (A) and sandwiched between 2 plates of 0.7 mm (B). The coolant was C_6F_{14} with an input temperature of -9.5 ^oC and flow 48.5 l/hr. The ambient temperature was ~ -11 ^oC, and the 'hybrid' was powered with a heat load of 4 W.

4.3 TPG-based thermal prototypes

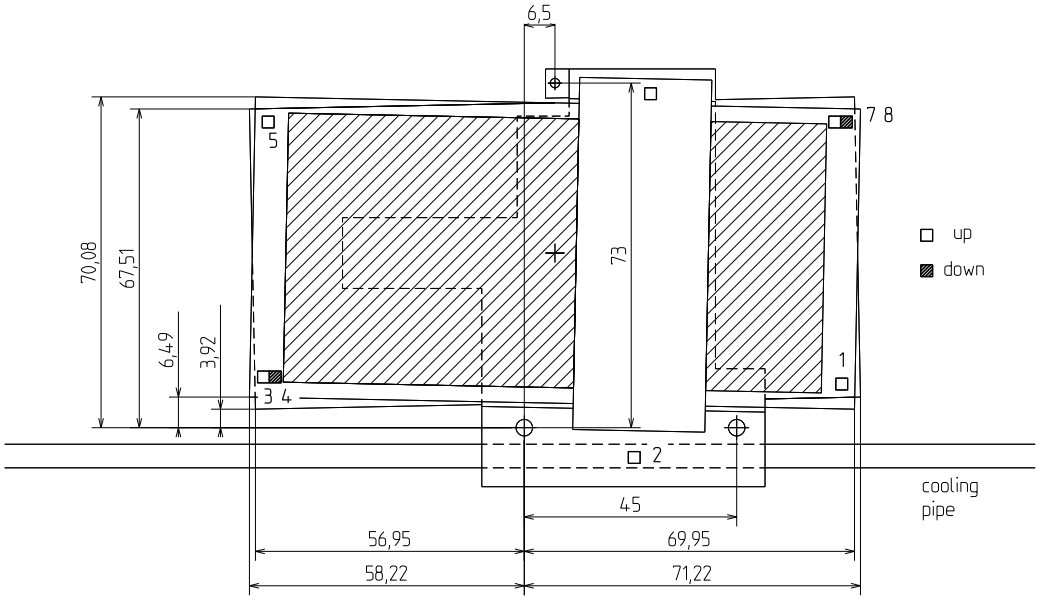

FIGURE 6. Layout and dimensions of the thermal module using all the materials of the base-line design. Also shown are the locations of PT100 sensors on the module.

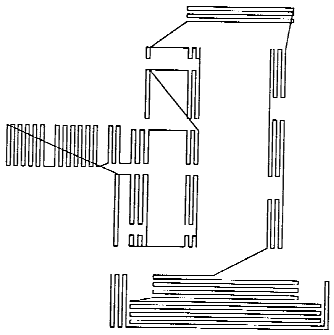

FIGURE 7. Glue layout (as obtained from RAL) for the araldite gluing of the TPG centre-piece to each silicon sensor

Detector Construction.

A total of four 'TPG-based' thermal modules (type C) have been made, and a fifth module is in preparation using irradiated CSEM silicon sensors instead of dummy silicon wafers with a glued heater pad.A further module (silicon sensors, TPG and BeO support pad only) has been fabricated for mechanical tests which are described in Section 4.4. Each of these modules attempts to exactly reproduce the thermal behaviour of barrel modules. The thermal module design is shown in Figure 6, and a photograph of module C-4 was shown in Figure 4. A schematic, shown in Figure 7, shows the glue pattern used for the glue dispenser. It is noted that the nominal glue thickness of 50 µm is too large for the glue pattern shown, and may have induced some un-glued areas (best checked using glass sensors). Table 5 lists the characteristics of each module.

Common elements	**• dummy silicon sensors of exact base-line dimension • TPG insert of base-line dimension and thickness • BeO hybrids of base-line design, fitted with 6 heater chips on each hybrid • BeO cooling contact and mechanical support • heater blanket on upper side (excepting module C-4)**
C-1	- equipped with PT100 sensors - glued using araldite 2011 with no filler, nominal thickness of 50 µm:
C-2	- mechanical module, not equipped with hybrid, heater pads, or PT100 sensors - glued using araldite 2011 with BN 140S filler (supplied by RAL) with proportion 2.5 gm resin: 2.0 gm hardener: 2.0 gm BN - glue thickness nominal 40 µm
C-3	- equipped with PT100 sensors - glued using araldite 2011 with BN 140S filler (supplied by RAL) with proportion 2.5 gm resin: 2.0 gm hardener: 1.93 BN - glue thickness of 40 µm on lower side but because of glue viscosity was 90µm on upper side
C-4	- equipped with PT100 sensors - glued using araldite 2011 with BN 140S filler (supplied by RAL) with proportion 2.5 gm resin: 2.0 gm hardener: 1.93 BN - glue thickness of 40 µm on each side
C-5	- under construction - dummy silicon replaced by irradiated barrel detectors (CSEM) - otherwise as for C-4

TABLE 5. Description of TPG-based thermal modules.

Operational Performance of Modules at Nominal Power Dissipation

Figure 8 shows a comparison of the thermal performance for module C-1, with a Cu-based thermal module, and with the Cu-based module A-5 as measured on the full length prototype discussed in Section 4.4. Apart from sensor #6 on the hybrid, which is expected to differ because of the different out-of-plane (i.e. thickness) heat conductivity, the results are in remarkable agreement.

The measured temperature profile of C-1 is significantly less good than a previous module reported in [2] (see Figures 15, 23 and 24 of that note) which had a significantly larger TPG surface. This is because the module of reference [2] was optimised for thermal behaviour, with the use of a TPG-based 'hybrid', and a TPG plate of 70 x 100 x 0.5 mm^3 was sandwiched between the detector planes.

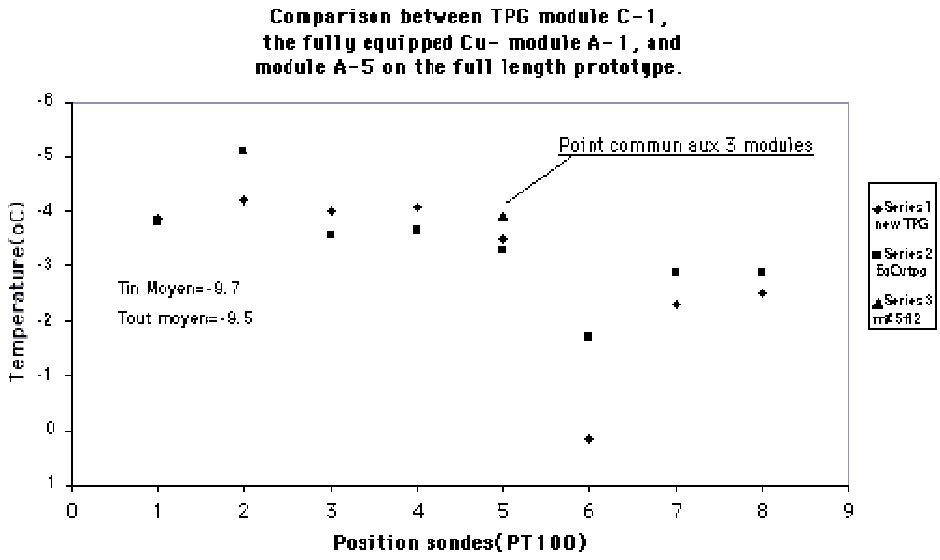

FIGURE 8. Comparison between TPG module C-1, the fully equipped Cu- module A-1, and module A-5 on the full length prototype.

Table 6 shows the temperature profile for the 3 TPG-based modules C-1, C-3 and C-4. For these measurements, the C_6F_{14} flow was 48 l/hour, with a pressure drop in the tube of ~ 290 mbars. The input coolant temperature was -10.03 ^oC. It is seen that significant temperature differences result from the changed glue characteristics of the 2 modules. Figure 9 shows the results for the case of 0.5 W sensor power and 4 W hybrid power.

Module #	Sensor 1	Sensor 2	Sensor 3	Sensor 4	Sensor 5	Sensor 6	Sensor 7	Sensor power
C-1	-4.33	-5.37	-4.85	-4.851	-4.85	-0.44	-3.29	0.5 W
C-3	-3.81	-5.37	-4.59	-5.11	-4.59	-1.48	-3.81	
C-4	-3.55	-5.11	-5.11	-5.11	-4.33	-1.74	-3.81	
C-1	-3.81	-5.11	-4.33	-4.33	-4.33	0.08	-2.77	0.75 W
C-3	-3.55	-5.11	-4.33	-4.59	-4.33	-1.22	-3.29	
C-4	-3.29	-4.85	-4.59	-4.59	-3.81	-1.22	-3.29	
C-1	-3.29	-4.85	-3.81	-3.81	-3.81	0.59	-2.26	1.0 W
C-3	-3.29	-4.85	-3.81	-4.01	-3.81	-0.70	-3.03	
C-4	-2.77	-4.59	-4.01	-4.01	-3.29	-0.;96	-2.77	
C-1	-2.77	-4.59	-3.03	-3.03	-3.03	1.11	-1.22	1.5 W
C-3	-2.51	-4.33	-3.03	-3.29	-2.77	-0.18	-2.26	
C-4	-2.0	-4.01	-3.29	-3.29	-2.52	-0.18	-2.0	

TABLE 6. Temperature profile of modules C-1 and C-4. The C_6F_{14} flow was 48 l/hour, with a tube pressure drop of ~ 290 mbars. The input coolant temperature was -10 ^oC. The hybrid power 4 W, and the sensor power is varied between 0.5 W and 1.5 W.

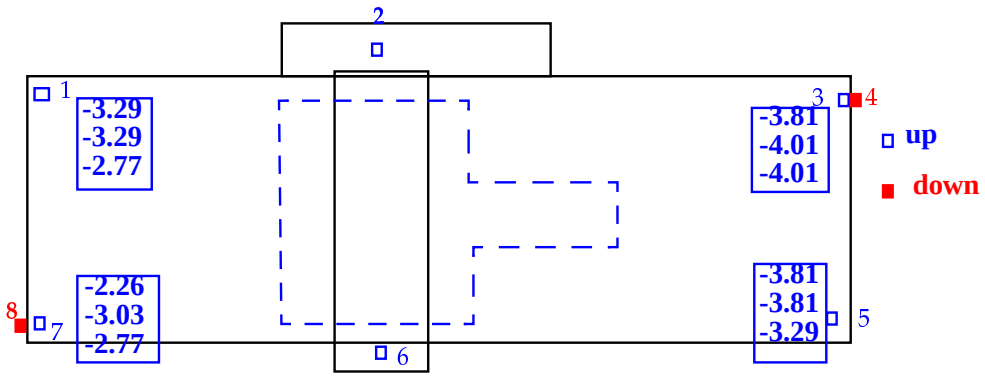

FIGURE 9. Measurements of the temperature at positions 1,3,5 and 7, for the TPG thermal modules C-1, C-3 and C-4, assuming a detector power of 1W. The measurements are as described in Table 6. A significant variation of temperature, for the modules, is evident.

Effect of Hybrid Power.

Because of the possibility of increased hybrid power consumption, measurements have been made in the Cu-based test module, the TPG-based module C-1 and the TPG-based module C-4, at hybrid power dissipations of between 4W and 8W.

These measurements have been made at a nominal coolant input temperature of -15 ^{o}C, with an ambient air temperature of both ~ -10 ^{o}C, and -15 ^{o}C.

Table 7 shows data for all 3 modules at T_{in} ~ -15 ^{o}C and T_{air} ~ -10^{o}C. A dependence of typically ~ 4 - 6 ^{o}C in the silicon temperature is measured by all sensors, for hybrid power variations of 4 W to 8 W. There is a much larger dependence on hybrid power for the hybrid itself (sensor #6). The hybrid temperature is evidently very sensitive to the thermal contact (glue?) between the hybrid and the cooling and support plate.

This indicates the necessity of a coolant at least 5-6 ^{o}C lower in temperature if the hybrid power increases significantly.

Table 8 shows that for module C-4, with a nominal hybrid power dissipation of 4 W, both the sensor *and* hybrid temperature is very sensitive to the ambient air temperature. This is shown graphically in Figure 10. We can conclude in a preliminary way that fluorinert cooling remains possible if the power consumption is increased, but both the coolant and ambient air temperatures should be significantly reduced. This effect is likely to be more pronounced in the more compact SCT environment.

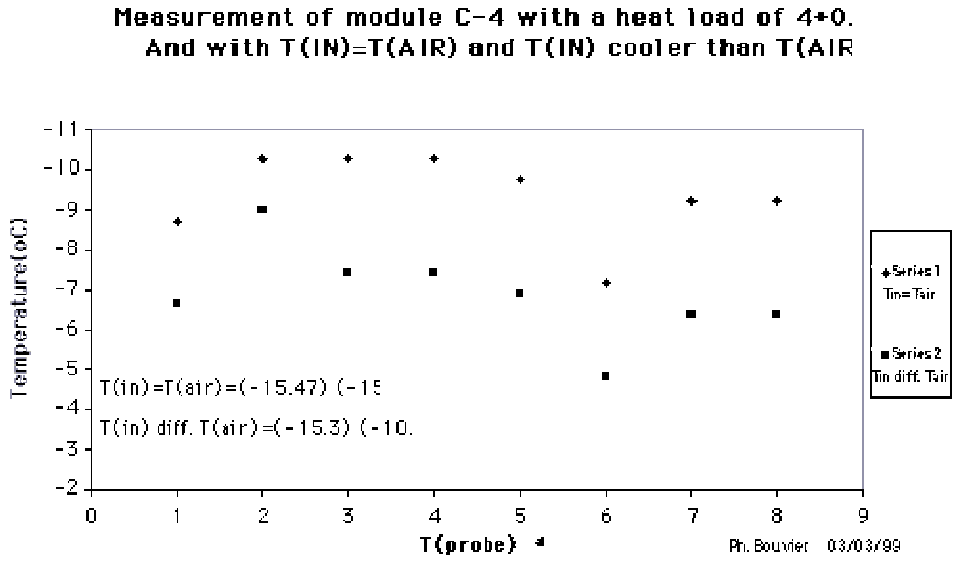

FIGURE 10. Dependence of C-4 module temperature on ambient air temperature for an input coolant temperature of -15 ^{o}C, and nominal heat dissipation of 4 W (hybrid) and 0.5 W (sensor).

Module #	Sensor 1	Sensor 2 (above cooling)	Sensor 3	Sensor 5	Sensor 6 (end hybrid)	Sensor 7	Heat load (W)
Cu	-8.5	-10.3	-8.7	-8.5	-6.9	-8.0	4 + 0.5 W
C-1	-7.2	-9.8	-8.0	-7.7	-4.0	-6.4	
C-3	-6.7	-9.0	-7.2	-6.7	-4.9	-6.4	
C-4	-6.7	-9.0	-7.4	-6.9	-4.9	-6.4	
Cu	-7.7	-9.8	-8.0	-7.4	-5.6	-6.9	5 + 0.5 W
C-1	-6.1	-8.5	-6.9	-6.4	-1.5	-4.9	
C-3	-5.4	-8.0	-6.1	-6.1	-3.0	-5.1	
C-4	-5.4	-8.0	-6.4	-5.6	-3.0	-4.9	
Cu	-6.4	-8.7	-6.7	-6.4	-4.5	-5.9	6 + 0.5 W
C-1	-5.1	-7.4	-5.9	-5.4	0.3	-3.6	
C-3	-4.3	-6.9	-5.4	-5.1	-1.2	-4.0	
C-4	-4.3	-6.9	-5.6	-4.6	-1.5	-3.8	
Cu	-5.6	-8.2	-5.9	-5.6	-2.8	-4.9	7 + 0.5 W
C-1	-4.0	-6.7	-4.9	-4.0	2.7	-1.7	
C-3	-3.0	-5.9	-4.0	-3.8	0.8	-2.5	
C-4	-3.0	-5.9	-4.6	-3.6	0.3	-2.5	
Cu	-4.6	-7.4	-4.9	-4.6	-1.2	-3.6	8 + 0.5 W
C-1	-2.8	-5.9	-3,6	-2.8	6.0	-0.2	
C-3	-2.0	-4.9	-3.0	-2.8	2.4	-1.0	
C-4	-2.0	-5.1	-3.8	-2.5	2.2	-1.5	

TABLE 7. Temperature profile of the Cu test module, and modules C-1 and C-4. The C_6F_{14} flow was 48.6 l/hour, with a pressure drop in the tube of ~320 mbars. The input coolant temperature was -15.3 ^{o}C, and the output temperature was -14.8 ^{o}C. The ambient air temperature was -10.03 ^{o}C. The hybrid temperature is evidently very fabrication dependent at high load.

Air Temperature	Sensor 1	Sensor 2 (above cooling)	Sensor 3	Sensor 5	Sensor 6 (end hybrid)	Sensor 7	
T_{air} = -15.2 °C	-8.74 (-8.99)	-10.3 (-10.3)	-10.3 (-9.77)	-9.77 (-9.77)	-7.18 (-6.4)	-9.26 (-8.74)	C-4 (C-3) T_{in} = -15.5 °C T_{out} = -14.9 °C ΔP = 320 mbar (typical)
T_{air} = -10.0 °C	-6.66 (-6.66)	-8.99 (-8.99)	-7.44 (-7.18)	-6.92 (-6.66)	-4.85 (-4.85)	-6.40 (-6.4)	
Difference	-2.08	-1.31	-2.76	-2.85	-2.33	-2.86	

TABLE 8. The effect on the module temperature of changing the ambient air temperature, for an ~ fixed input coolant liquid, and coolant pressure. Sensor 1 is closest to the cooling contact.

4.4 Mechanical measurements of a silicon-TPG sandwich.

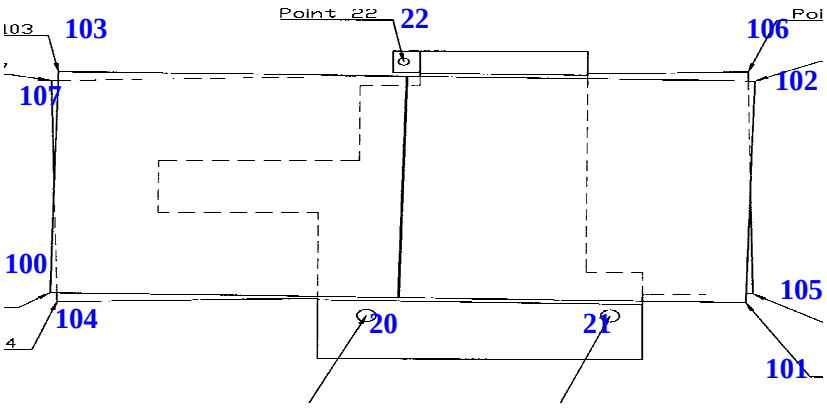

FIGURE 11. Schematic of the mechanical barrel module, with the measurement points 20-22 and 100-107 shown.

The module C-2 was built in principle according to mechanical specifications. The module was then measured (in a 2-dimensional projection) by a Mitutoyo Euro-C9106 measuring machine. Two independent measurements for points 20-22 and 101-107 (Figure 11) were initially made, and the means of these measurements are listed in Table 9.

The module was then temperature cycled twice between -10°C and +40°C, and subsequently allowed to return to the ambient temperature of ~ 21°C. It was then re-measured, and the results are again shown in Table 9, again as projected to the nominal z-value z=0.

Even after ignoring the measurement 103 which is a clear anomaly., the deviations measured are not marginal, and further measurements will be made.

Measurement Point	Before thermal cycling		After thermal cycling		Difference	
	x (mm)	y (mm)	x (mm)	y (mm)	δx (µm)	δy (µm)
20	0.0005	0.000	-0.0015	0.001	-1.0	+1.0
21	44.975	-0.001	44.9785	-0.0005	+3.5	+0.5
22	6.473	73.026	6.476	73.021	+3.0	-5.0
100	-58.17715	6.492	-58.1595	6.4935	+12.0	+1.5
101	69.996	4.0015	69.998	3.9955	+2.0	-6.0
102	71.248	67.586	71.2555	67.581	+7.5	-5.0
103	-56.9545	70.075	-56.9185	70.045	+36.0	-30.0
104	-56.969	3.9325	-56.9715	3.929	-2.5	-3.5
105	71.224	6.5885	71.226	6.5815	+2.0	-7.0
106	69.9455	70.1695	69.9495	70.1635	+4.0	-6.0
107	-58.2785	67.516	-58.278	69.5115	+0.5	-4.5

TABLE 9. Measured position of barrel module C-2 before and after temperature cycling (July 1998).

4.5 The Full Length Prototype Support Structure.

Figure 12 shows a photograph of the full length support structure used for cooling tests. The figure shows a single oval cooling tube support on carbon fibre support brackets of the base-line design. The support can be equipped with up to 2 rows of thermal modules, therefore permitting a 'system test' of thermal behaviour. The figure shows a detail of the mounting bracket, with a Cu-based module mounted on a 2nd bracket.

Figure 13 shows the same structure, with modules mounted in a castellated way (high or low) as in the base-line design. Figure 14 and Table 10 show the temperature of each module (sensor #5 as described above) when all 12 Cu-modules are attached to the mounting brackets (with a heat contact of 50 µm conductive grease).

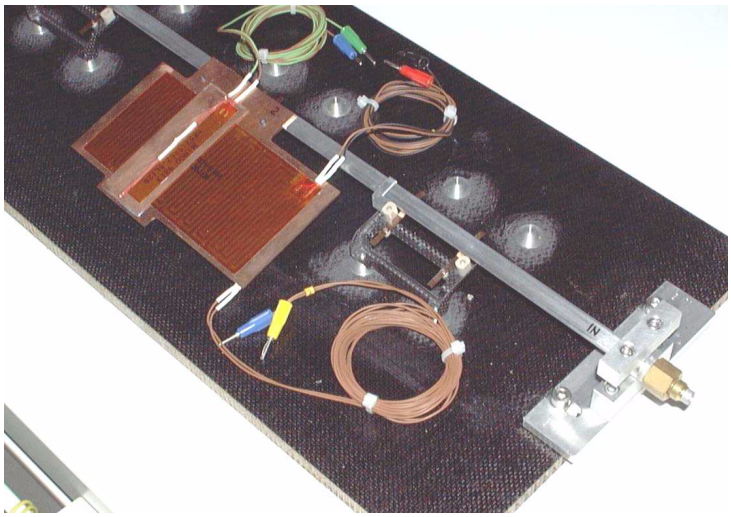

FIGURE 12. Photo of support structure, showing a detail of the bracket and oval cooling tube, and a Cu-based module attached to a 2nd bracket.

FIGURE 13. Full length prototype, fully equipped with one row of Cu-based thermal modules

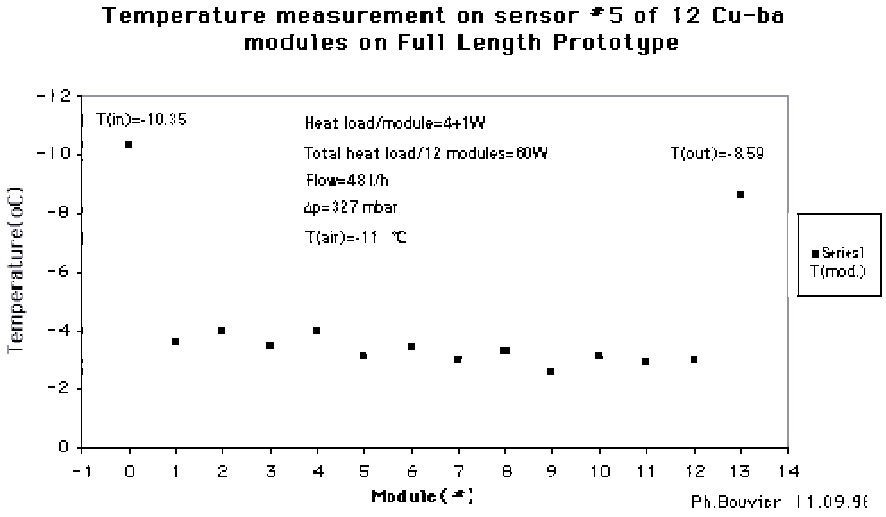

FIGURE 14. Temperature recorded on sensor #5 of each of 12 Cu- thermal modules described above, attached to brackets of the full length prototype structure.

These results show an excellent uniformity of the module temperature. Modules attached in the high position have a temperature difference with respect to the tube of 6.43 ^{o}C, with an rms spread of only 0.24 ^{o}C. Modules attached in the low position have a mean temperature of 5.95 ^{o}C, a difference of 0.48 ^{o}C, with an rms spread of 0.16 ^{o}C. Given the previous module-to-module comparison, the temperature spread is ascribed to differences of the heat contact.

Stability of the module position following temperature cycling.

In the existing base-line barrel design, the longitudinal temperature expansion coefficient of the oval aluminium tube (23 ppm/^{o}C) is significantly different from that of the module, with 2 mounting points from a BeO base plate (4 ppm/^{o}C) mounted on a carbon fibre bracket and an overall support structure which has a CTE of < 1 ppm/^{o}C.

It is therefore important to ensure, during warm-up and cool-down, that the tube movement does not introduce an uncontrolled module movement. Preliminary results, which must be repeated with better precision, indicate that this is the case.

The cooling tube (length 1.52 m), which was mounted on the carbon fibre brackets as in Figure 6. It was fixed at the coolant inlet side, and left free to move longitudinally at the other end, as in the SCT engineering design. A total of 12 modules were mounted on the structure, in thermal contact with the cooling tube. The longitudinal position of the end module, and of the aluminium movement, was measured in successive temperature cycles, as shown in Table 11. Within the measurement accuracy, there was no module movement, although there is some evidence of a reduced effective CTE for the tub (possibly due to differing liquid and tube temperatures). This result must be checked with improved accuracy on a long-term basis, using the final cooling design. In parallel, attempts will be made to reduce the CTE of the aluminium tube [7].

Coolant C_4F_{10} **Flow rate** 48 l/hr **ΔP** 327 mbar **T (freezer)** -11.1 °C **ΔT (in - out)** -1.76 °C		
Module # and orientation	**T °C (sensor 5)**	**ΔT (tube-sensor) °C (linear corrected)**
T_{in}	-10.35	
A-1 H	-3.6	6.61
A-2 L	-3.98	6.10
A-3 H	-3.47	6.47
A-4 L	-3.96	5.85
A-5 H	-3.13	6.54
A-6 L	-3.4	6.14
A-7 H	-2.97	6.43
A-8 L	-3.26	6.01
A-9 H	-2.58	6.55
A-10 L	-3.1	5.90
A-11 H	-2.91	5.95
A-12 L	-3.01	5.71
T_{out}	-8.59	
<ΔT (high)> 6.42 °C rms 0.24 °C **<ΔT (low)> 5.95 °C rms 0.16 °C**		

TABLE 10. Temperature measurement of 12 Cu-based thermal modules attached to the support structure of the full length prototype.

$T_{initial}$ °C	T_{final} °C	ΔT °C	δl_{meas} Al (mm)	δl_{theory} Al (mm)	δl_{meas} module (mm)	δl_{theory} module (mm)
-10	28	38	1.19	1.32	-	-
28	-10	38	-1.21	-1.32	0.01	0.0
-10	28	38	1.19	1.32	0.01	0.0

TABLE 11. Measurements of the distortion in module position induced by temperature variations.

5.0 Summary

In the above sections, we have provided a summary of existing results using the full-length thermal prototype. The following conclusions can be made:

- Over-pressure single phase cooling using the oval pipe solution on the barrel appears feasible, albeit with high flow rates for fluorcarbon coolants.
- Grease contacting of the detectors to the pipe appears reliable and reproducible. Long term cycling tests are required.
- The mechanical stability of the barrel module after temperature cycling is marginal, and more measurements are required (including long term stability measurements).
- When a decision is made on the final coolant and pipe dimensions, etc., the full length prototype will be modified accordingly.
- At the present time, 3 base-line TPG-based thermal modules manufactured by the University of Geneva are available for comparative tests. It would be very useful to compare these results, directly on the same full-length prototype set-up, with modules fabricated in other institutes.
- Simulation studies are urgently needed.

References

1 ATLAS Inner Detector Technical Design Report, CERN/LHCC/97-16, and 97-17.

2 G. Barbier et al., Status Report on module cooling and mechanics, ATLAS INDET-NO-166 (17 April 1997).

3 Interim Report on a Review of ATLAS Cooling Systems, ATL-TC-EN-007 (1997), ed. M. Hatch.G. Hallewell et al.

4 G. Hallewell, presentation at ATLAS SCT Week, February 1999. See http://www.cern.ch/Atlas/GROUPS/INNER_DETECTOR/SCT/sct_meetings.html.

5 O. Gildemeister, see RD2 Status Report to the DRDC, CERN/DRDC/92-4 (January 1992), and CERN/DRDC/94-34 (August 1994). See also the CMS Inner Detector Technical Design Report.

6 Ongoing activities of the CERN Cooling Group towards an evaporative cooling for the SCT and Pixel detectors.

7 This involves the gluing of ~0-CTE carbon fibres along the full length of the aluminium tube. The idea was originally proposed by the Nikhef Group.

8 Report on evaporative cooling. In preparation.